JACS
JOURNAL OF THE AMERICAN CHEMICAL SOCIETY
Communication
pubs.acs.org/JACS

Styrene Purification by Guest-Induced Restructuring of Pillar[6]arene

Kecheng Jie,[†,§] Ming Liu,[‡,§] Yujuan Zhou,[†] Marc A. Little,[‡] Satyanarayana Bonakala,[‡] Samantha Y. Chong,[‡] Andrew Stephenson,[‡] Linjiang Chen,[‡] Feihe Huang,*[,†] and Andrew I. Cooper*[,‡]

[†]State Key Laboratory of Chemical Engineering, Center for Chemistry of High-Performance & Novel Materials, Department of Chemistry, Zhejiang University, Hangzhou 310027, P. R. China

[‡]Department of Chemistry and Materials Innovation Factory, University of Liverpool, Crown Street, Liverpool L69 7ZD, U.K.

Supporting Information

ABSTRACT: The separation of styrene (**St**) and ethylbenzene (**EB**) mixtures is important in the chemical industry. Here, we explore the **St** and **EB** adsorption selectivity of two pillar-shaped macrocyclic pillar[*n*]arenes (**EtP5** and **EtP6**; *n* = 5 and 6). Both crystalline and amorphous **EtP6** can capture **St** from a **St**-**EB** mixture with remarkably high selectivity. We show that **EtP6** can be used to separate **St** from a 50:50 v/v **St**:**EB** mixture, yielding in a single adsorption cycle **St** with a purity of >99%. Single-crystal structures, powder X-ray diffraction patterns, and molecular simulations all suggest that this selectivity is due to a guest-induced structural change in **EtP6** rather than a simple cavity/pore size effect. This restructuring means that the material "self-heals" upon each recrystallization, and **St** separation can be carried out over multiple cycles with no loss of performance.

Styrene (**St**) is an important aromatic feedstock in the chemical industry.[1] More than 80% of **St** production is used for polymerization or copolymerization to produce thermoplastics, synthetic rubbers, and resins. **St** is mainly produced by dehydrogenation of ethylbenzene (**EB**):[2] after dehydrogenation, the product stream still contains a large fraction (20−40%) of unreacted **EB** that must be removed.[3] Separation by conventional distillation on an industrial scale is not practical because of the small difference in boiling point (9 K) between **St** (bp 418.3 K) and **EB** (bp 409.3 K). Currently, the preferred technology is extractive distillation and vacuum distillation, performed in the presence of polymerization inhibitors like phenylene-diamines or dinitrophenols.[5] However, this is energetically intensive and most of the energy used in the production of **St** can be accounted for by the separation process. Also, small amounts of impurities with similar boiling points such as toluene (bp 393 K) and *o*-xylene (bp 418 K) must also be removed from the **St**-**EB** product stream, further complicating the procedure.[3,4]

An alternative and potentially more energy-efficient separation strategy is to exploit the molecular, chemical, and geometrical differences of **St** and **EB** in an adsorptive separation, for example by using nanoporous materials such as metal−organic frameworks (MOFs) or zeolites.[5−10] Adsorptive technologies do not require elevated temperatures, and hence the problem of side reactions can be circumvented, providing that the adsorbent itself is not reactive. However, the molecular sizes of **St** and **EB** are very similar (Figure 1a), making it difficult to find a suitable

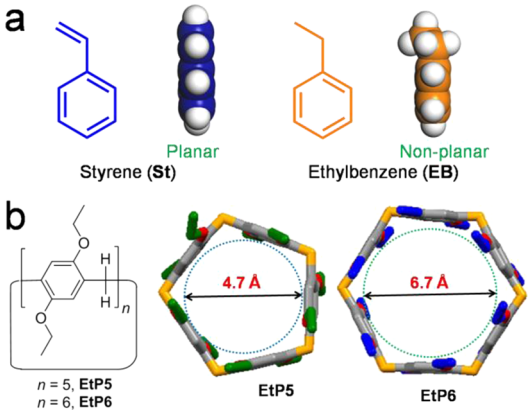

Figure 1. Chemical structures: (a) **St** and **EB**; (b) **EtP5** and **EtP6**. The internal cavity diameters of **EtP5** and **EtP6** are based on the inscribed circle of the regular pentagon and hexagon, respectively.

porous material for their separation. In principle, crystallization-based separations can also be energy efficient. Unlike adsorptive separation, which uses materials with pre-existing pores, the "pores" in crystallization separation are created during assembly of the crystalline inclusion compound. These "pores" are generally only stable when occupied by guest molecules.[11] To our knowledge, no such separation method has been reported for styrene purification.

Pillar[*n*]arenes (*n* = 5−15) were first reported in 2008 as a novel class of supramolecular host.[12−22] The host−guest properties of pillar[*n*]arenes have been investigated intensively and they have been applied in the fabrication of various supramolecular systems, such as interlocked structures, molecular machines, supramolecular polymers, and supramolecular amphiphiles.[12−20] There are only a few occasions where pillar[*n*]arenes have been used as solid materials. For example, Yang et al. reported a pillar[5]arene-based supramolecular organic framework which has selective adsorption of CO_2 over N_2 at room temperature.[21] Ogoshi et al. reported that a pillar[5]arene functionalized with ethyl groups could encapsulate *n*-alkanes in its cavity in the solid state.[22]

Here, we investigate two pillararenes with different cavity sizes, perethylated pillar[5]arene (**EtP5**) and pillar[6]arene (**EtP6**) (Figure 1b), as adsorptive separation materials to separate **St** and **EB**. We show that both crystalline and amorphous **EtP6** can

Received: December 27, 2016
Published: February 9, 2017

DOI: 10.1021/jacs.6b13300
J. Am. Chem. Soc. 2017, 139, 2908−2911

selectively capture **St** from a mixture of **St** and **EB**. The adsorbed **St** molecules are located in the extrinsic pores between distorted **EtP6** molecules in a crystal structure that transforms to accommodate the **St** guest. The separation process for **EtP6** is a solid-state recrystallization separation, rather than an adsorptive separation. This process is quite different from separations that use porous adsorptive materials such as MOFs or zeolites, where intrinsic pore size and shape plays the determining role.

EtP5 and **EtP6** were synthesized by a previously reported method.[19] Single crystals of **EtP5** and **EtP6** loaded with **St** and **EB** were obtained by slow evaporation of a **St** or **EB** solution of the pillararene, respectively. Despite numerous attempts, no diffractable single crystals could be grown of **St**-loaded **EtP5**. By contrast, **EB** forms a 1:1 host–guest complex with **EtP5** (**EB@EtP5**; Figure 2a, left). In **EB@EtP5**, an **EB** molecule is threaded

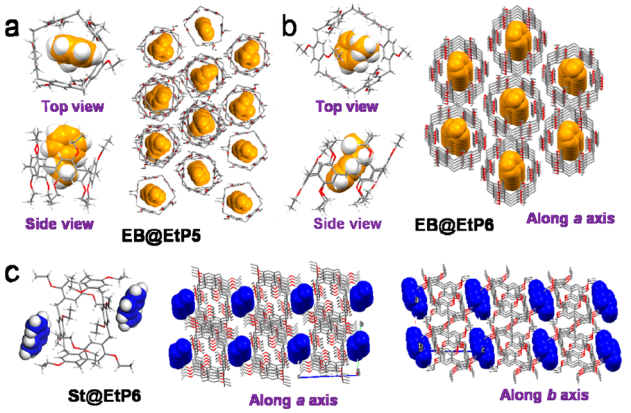

Figure 2. Single-crystal structures: (a) **EB@EtP5**; (b) **EB@EtP6**; and (c) **St@EtP6**. **St** is accommodated in 2D extrinsic channels *between* the pillararenes in **St@EtP6**.

into the cavity of **EtP5** with its ethyl group in the cavity center. This gives rise to CH···π interactions between the ethyl group on **EB** and the benzene rings on **EtP5**. The pentagonal structure of **EtP5** forms infinite 1D channels with **EB** in the channels (Figure 2a, right). In the analogous solvated crystal structure of **EtP6** (**EB@EtP6**), an **EB** molecule is located in the center of the cavity. This is stabilized by π–π stacking between **EB** and benzene rings on **EtP6**, also forming a 1:1 host–guest complex (Figure 2b, left). The hexagonal pillar structure of **EtP6** contributes to the formation of infinite intrinsic diagonal 1D channels with **EB** in the channels (Figure 2b, right). The solvated crystal structure of **EtP6** with **St** (**St@EtP6**) is markedly different. Two opposite repeating units of **EtP6** are turned perpendicular to their adjacent units, giving **EtP6** a more deformed hexagonal structure with a cavity that is too small to accommodate a **St** guest molecule (Figure 2c, left). However, the **EtP6** molecule does form infinite extrinsic 2D channels between the macrocycles along the *a* and *b* axes, with **St** molecules accommodated in these channels (Figure 2c, middle and right).

From these three crystal structures alone, it might be expected that **EtP6** has potential to selectively capture **EB** from a **St**-**EB** mixture due to its good fit in the **EtP6** intrinsic cavity. Solid–vapor adsorption experiments were performed to test this. Desolvated crystalline **EtP5** (**EtP5**α) and **EtP6** (**EtP6**α) were first prepared as adsorptive materials (for details, see the Supporting Information). Neither **EtP5**α nor **EtP6**α showed significantly different adsorption rates for **St** or **EB** vapor (Figures S7 and S9). For **EtP5**α, **EB** was adsorbed slightly faster than **St** whereas **EtP6**α adsorbed both **St** and **EB** at similar rates. The major difference is the amount of **St** and **EB** adsorbed by **EtP6**α, which is much higher than **EtP5**α (Figure S7). To monitor the adsorption of neat **St** and neat **EB** by **EtP5**α and **EtP6**α, we carried out *in situ* PXRD studies. The PXRD patterns of **EtP5**α did not change after adsorption of **St** or **EB**, indicating that the structure of **EtP5**α did not change after exposure to **St** or **EB** (Figure S8). We concluded that **EB** or **St** was not, in fact, adsorbed in the bulk by **EtP5**α. Instead, we ascribe the small, substoichiometric uptake of **St** (and **EB**) by **EtP5**α to surface adsorption on the crystals. By contrast, the PXRD patterns of **EtP6**α after adsorption of **St** or **EB** were different from **EtP6**α and in good agreement with the simulated PXRD patterns for **St@EtP6** and **EB@EtP6**, respectively (Figure S9b). Hence, the adsorption of **St** or **EB** by **EtP6**α triggers a crystal transformation from **EtP6**α to **St@EtP6** or **EB@EtP6**, respectively (Figure S9c). **EtP6** is thus a more promising material than crystalline **EtP5** for the capture of **St** or **EB**.

To investigate whether **EtP6**α could discriminate between a mixture of **EB** and **St**, we carried out time-dependent **EtP6**α solid–vapor sorption experiments for a **St**-**EB** mixture (the **St**-**EB** mixture used is always 50:50 v/v). The uptake rates of **St** and **EB** in **EtP6**α were essentially the same over the first hour (Figure 3a). Surprisingly, however, the uptake of **St** increased

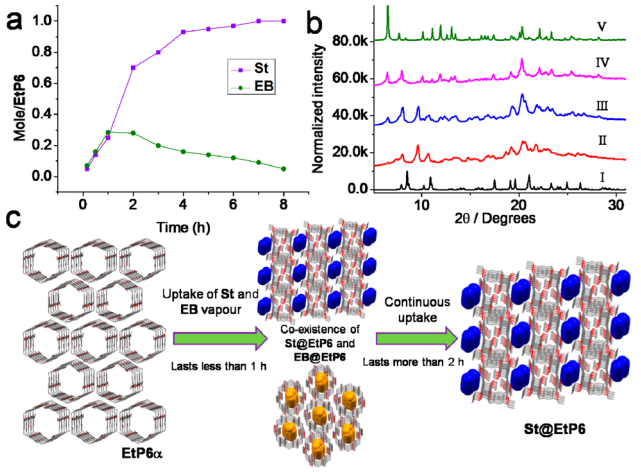

Figure 3. (a) Time-dependent **EtP6**α solid–vapor sorption plot for **St**-**EB** mixture vapor. (b) Time-dependent PXRD patterns of **EtP6**α: (I) simulated from single-crystal structure of **EB@EtP6**; after adsorption of **St**-**EB** mixture vapor for (II) 1 h, (III) 2 h, and (IV) 8 h; (V) simulated PXRD pattern from single-crystal structure of **St@EtP6**. (c) Representation of **EtP6**α structural changes upon uptake of **St**-**EB** mixture vapor.

dramatically after the first hour and quickly increased to approximately 1 mol/**EtP6** after 4 h. The uptake of **EB** slowly decreased after the first hour, presumably because it was being displaced by **St** molecules and forced out of the intrinsic cavity as the structural transformation occurred. Gas chromatography was used to deduce the ratio of **St** and **EB** adsorbed by **EtP6**α over the course of the experiment (Figures S10 and S11). This showed that **EtP6**α could selectively capture **St** from a **St**-**EB** mixture, contrary to our initial hypothesis that **EB** might be selectively adsorbed. A time-dependent PXRD experiment was performed to monitor the transformation of **EtP6**α after exposure to a **St**-**EB** mixture (Figure 3b). Comparison of the PXRD pattern recorded after adsorption of the **St**-**EB** mixture

DOI: 10.1021/jacs.6b13300
J. Am. Chem. Soc. 2017, 139, 2908–2911

vapor for 1 h with the simulated profiles of **St@EtP6** and **EB@EtP6** suggests the coexistence of **St@EtP6** and **EB@EtP6** phases after the initial exposure period (Figure S12). With increasing adsorption time, the PXRD pattern becomes more like **St@EtP6** until it becomes fully consistent with the **St@EtP6** structure. A putative mechanism, consistent with these observations is as follows: initially, the uptake rates of both **St** or **EB** in **EtP6***α* are similar, and both **St** and **EB** can occupy empty **EtP6***α* crystals, transforming them into two new polymorphs, **St@EtP6** and **EB@EtP6**. However, **St@EtP6** is more stable than **EB@EtP6**, and over time, **St** molecules diffuse into **EB@EtP6**, displacing **EB** molecules and transforming **EB@EtP6** into **St@EtP6**.

We then carried out additional time-dependent solid−vapor sorption experiments using **EB**-loaded **EB@EtP6** and **St**-loaded **St@EtP6** to further investigate this guest-induced structural transformation. The uptake of **St** increased rapidly within 1 h when a **St-EB** vapor mixture was diffused into preloaded **EB@EtP6** (Figure 4a). A saturation point was reached after

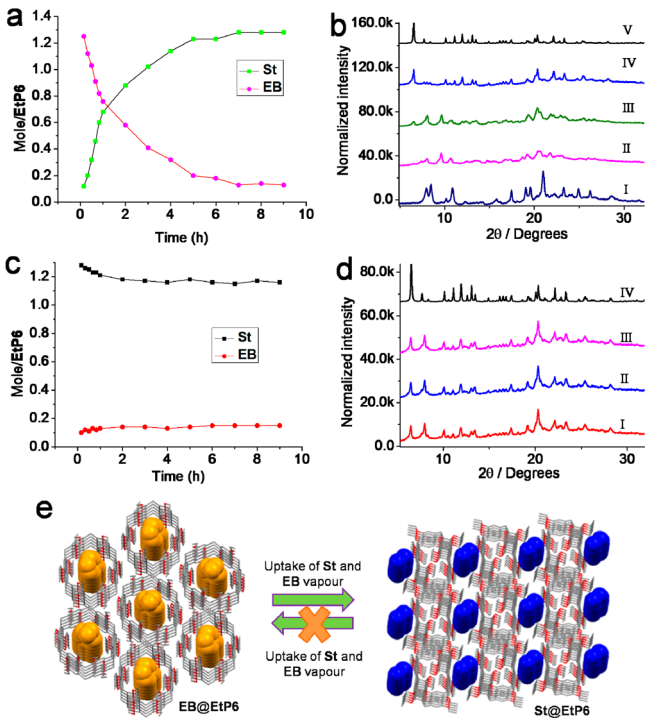

Figure 4. (a) Time-dependent **EB@EtP6***α* solid−vapor sorption plot for **St-EB** mixture vapor. (b) Time-dependent PXRD patterns of **EB@EtP6**: (I) original **EB@EtP6**; after adsorption of **St-EB** mixture vapor for (II) 1 h, (III) 2 h and (IV) 8 h; (V) simulated from single-crystal structure of **St@EtP6**. (c) Time-dependent **St@EtP6***α* solid−vapor sorption plot for **St-EB** mixture vapor. (d) Time-dependent PXRD patterns of **St@EtP6**: (I) original **St@EtP6**; after adsorption of **St-EB** mixture vapor for (II) 1 h and (III) 8 h; (IV) simulated from single-crystal structure of **St@EtP6**. (e) Structural representation of the irreversible transformation between **St@EtP6** and **EB@EtP6** upon uptake of **St-EB** mixture vapor.

about 7 h. **EB**, which was originally located in the 1D channels of **EB@EtP6**, was displaced by **St** and its loading decreased as the **St** content increased. Time-dependent PXRD patterns (Figure 4b) indicate the guest-induced crystal-to-crystal transformation from **EB@EtP6** to **St@EtP6** over time. Hence, even when **EB** molecules were fully preloaded into crystals of **EtP6**, **St** molecules in the **St-EB** mixture can penetrate these crystals and replace **EB**. By contrast, when fully solvated **St@EtP6** is exposed to the mixture of **St-EB** vapor, these crystals maintain a high loading of **St** and the **EB** uptake is negligible (Figure 4c). As expected, the PXRD pattern did not change at all, indicating that **EB** molecules in the **St-EB** mixture cannot replace **St** molecules in **St@EtP6** (Figure 4d,e). This suggests that the **St@EtP6** phase is more thermodynamically stable than the **EB@EtP6** phase.

To rationalize this, we performed electronic density functional theory calculations to understand the structural stability of three **EtP6** structures loaded with styrene molecules, i.e., (1) the experimental **St@EtP6** phase; (2) the experimental **EB@EtP6** phase with **EB** replaced by **St**, and; (3) the experimental **EtP6***α* phase with **St** artificially inserted (the molar ratio of **St** and **EtP6** = 1:1; **St** molecules were placed at the center of each **EtP6**). Table S4 summarizes the lattice energies determined for these three styrene-loaded structures. The experimentally observed **St@EtP6** structure has the lowest lattice energy (−529 kJ/mol) among the three polymorphs, explaining its preferred formation.

To show that **EtP6** has practical potential for styrene purification, we developed a procedure to obtain **St** with high purity from a **St-EB** mixture using crystalline **EtP6** as the adsorbent. After adsorption of a **St-EB** vapor mixture, crystalline **EtP6** was heated at 40 °C for 30 min to remove any unbound **St** or **EB** molecules adsorbed on the crystal surface. **St** could then be released from the selectively formed **St@EtP6** phase with a purity of over 99% (Figure 5b).

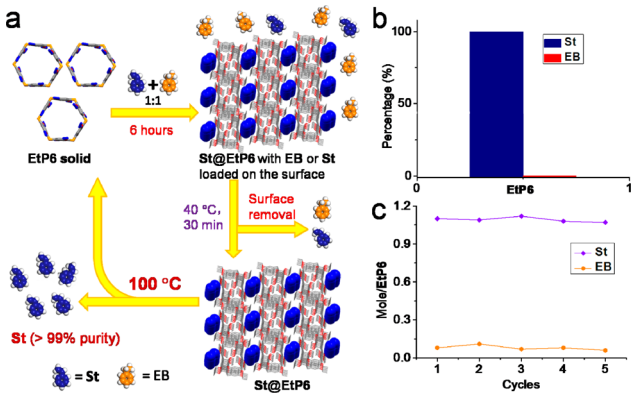

Figure 5. (a) Schematic representation of the general method to obtain highly pure **St** from a **St-EB** mixture using **EtP6** as the adsorbent and the recycling of **EtP6**. (b) Relative amount of **St** and **EB** in the resultant vapor measured by gas chromatography. (c) Maximum uptake of **St** and **EB** in **EtP6** for 6 h after the same material is recycled five times.

One bane of adsorbent technology is decreased performance over time, because of either instability of the porous framework or fouling. To be practically useful, an adsorbent must perform well over multiple cycles without any degradation. Thus, an important question was whether the resultant desolvated **EtP6** crystals can still selectively capture **St** from a **St-EB** mixture in a second cycle, after **St** is completely removed from the **St@EtP6** crystals. Indeed, the desolvated **St@EtP6** was shown by PXRD experiments to be a new polymorph, **EtP6***β* (Figure S17). Nonetheless, time-dependent solid−vapor experiments using the same **St-EB** vapor mixture showed that **EtP6***β* has adsorption properties for **St** and **EB** that are just like **EtP6***α*, indicating that **EtP6***β* can also selectively capture **St** from a **St-EB** mixture (Figure S20). PXRD experiments suggest the same selectivity mechanism as **EtP6***α* and **EB@EtP6** (Figure S21). Since the selectivity seems to be unaffected by this polymorphism in **EtP6**, we further investigated whether amorphous **EtP6** might also

DOI: 10.1021/jacs.6b13300
J. Am. Chem. Soc. 2017, 139, 2908−2911

have the same performance. Adsorption and PXRD experiments showed that amorphous **EtP6** could also selectively adsorb **St** (Figures S24 and S25). As such, it is not necessary to use crystalline **EtP6** for styrene purification and **EtP6** can be recycled multiple times without losing its styrene selectivity or adsorption capacity (Figure 5c). Effectively, this crystallization route is a "self-healing" system: the separation works irrespective of the starting **EtP6** structure. This is different from processes involving extended porous frameworks where loss of porosity or phase changes are often irreversible and catastrophic.

In summary, we have investigated the adsorptive properties of two easily obtained pillar[*n*]arenes, **EtP5** and **EtP6**, toward **St** and **EB**. **EtP6** was found to be a much better absorbent for both **St** and **EB**, and either crystalline or amorphous **EtP6** can selectively capture **St** from a **St**-**EB** mixture. This selectivity arises from the guest-induced selective structural change of **EtP6** rather than the suitable cavity size. Compared with other small molecule organic separation materials, such as intrinsically porous cage compounds,[23] the separation process for **EtP6** is closer to a crystallization separation, rather than an adsorptive separation. While the separation of **St** and **EB** has been achieved in porous extended frameworks, such as MOFs, this new molecular approach offers potential advantages. For example, **EtP6** is soluble, is easy to synthesize, and has better chemical stability than many crystalline MOFs and COFs. While the overall uptake capacity in **EtP6** is relatively low compared with porous extended frameworks, and the uptake kinetics are relatively slow, **St** can be separated with high purity in just one cycle, which is highly desirable. Future work will attempt to increase the uptake capacity and adsorption kinetics without losing the remarkable selectivity, for example by cocrystallization of two or three different pillar[*n*]arenes. Other hydrocarbon separations, such as the separation of xylene isomers, are also under investigation.

■ ASSOCIATED CONTENT

Supporting Information

The Supporting Information is available free of charge on the ACS Publications website at DOI: 10.1021/jacs.6b13300.

Experimental details, crystallography, and other materials, including Figures S1−S25 and Tables S1−S4 (PDF)

X-ray crystallographic data for 2(EtP5)·4(THF), EB@EtP5, EtP6·3(acetone), EB@EtP6, and St@EtP6 (CIF)

■ AUTHOR INFORMATION

Corresponding Authors

*fhuang@zju.edu.cn

*aicooper@liverpool.ac.uk

ORCID

Samantha Y. Chong: 0000-0002-3095-875X

Feihe Huang: 0000-0003-3177-6744

Author Contributions

§K.J. and M.L. contributed equally to this work.

Notes

The authors declare no competing financial interest.

■ ACKNOWLEDGMENTS

This work was supported by the National Basic Research Program (2013CB834502), the National Natural Science Foundation of China (21434005, 91527301), and the Open Project of State Key Laboratory of Supramolecular Structure and Materials (sklssm201611). The authors gratefully acknowledge the Engineering and Physical Sciences Research Council (EP/K018396/1 and EP/N004884/1) and European Research Council under the European Union's Seventh Framework Programme/ERC Grant Agreement no. [321156] for financial support.

■ REFERENCES

(1) *Kirk-Othmer Encyclopedia of Chemical Technology*; John Wiley & Sons, Inc.: New York, 2008; pp 1040.

(2) *Ullmann's Encyclopedia of Industrial Chemistry*, 6th ed.; John Wiley & Sons, Inc.: New York, 2006; electronic release.

(3) Butler, J. R.; Watson, J. M.; Forward, C. H. U.S. Patent 4417085, 1983.

(4) Berg, L. U.S. Patent 4959128, 1990.

(5) Ahmad, R.; Wong-Foy, A. G.; Matzger, A. J. *Langmuir* **2009**, *25*, 11977.

(6) Maes, M.; Alaerts, L.; Vermoortele, F.; Ameloot, R.; Couck, S.; Finsy, V.; Denayer, J. F. M.; De Vos, D. E. *J. Am. Chem. Soc.* **2010**, *132*, 2284.

(7) Maes, M.; Vermoortele, F.; Alaerts, L.; Couck, S.; Kirschhock, C. E. A.; Denayer, J. F. M.; De Vos, D. E. *J. Am. Chem. Soc.* **2010**, *132*, 15277.

(8) Remy, T.; Ma, L.; Maes, M.; De Vos, D. E.; Baron, G. V.; Denayer, J. F. M. *Ind. Eng. Chem. Res.* **2012**, *51*, 14824.

(9) Yang, C.-X.; Yan, X.-P. *Anal. Chem.* **2011**, *83*, 7144.

(10) Smit, B.; Maesen, T. *Nature* **1995**, *374*, 42.

(11) Pivovar, A. M.; Holman, K. T.; Ward, M. D. *Chem. Mater.* **2001**, *13*, 3018.

(12) Ogoshi, T.; Kanai, S.; Fujinami, S.; Yamagishi, T.; Nakamoto, Y. *J. Am. Chem. Soc.* **2008**, *130*, 5022.

(13) Ogoshi, T.; Yamagishi, T.-a.; Nakamoto, Y. *Chem. Rev.* **2016**, *116*, 7937.

(14) Han, C.; Ma, F.; Zhang, Z.; Xia, B.; Yu, Y.; Huang, F. *Org. Lett.* **2010**, *12*, 4360.

(15) Cao, D.; Kou, Y.; Liang, J.; Chen, Z.; Wang, L.; Meier, H. *Angew. Chem., Int. Ed.* **2009**, *48*, 9721.

(16) Si, W.; Chen, L.; Hu, X.-B.; Tang, G.; Chen, Z.; Hou, J.-L.; Li, Z.-T. *Angew. Chem., Int. Ed.* **2011**, *50*, 12564.

(17) Strutt, N. L.; Fairen-Jimenez, D.; Iehl, J.; Lalonde, M. B.; Snurr, R. Q.; Farha, O. K.; Hupp, J. T.; Stoddart, J. F. *J. Am. Chem. Soc.* **2012**, *134*, 17436.

(18) Yu, G.; Xue, M.; Zhang, Z.; Li, J.; Han, C.; Huang, F. *J. Am. Chem. Soc.* **2012**, *134*, 13248.

(19) Hu, X.-B.; Chen, Z.; Chen, L.; Zhang, L.; Hou, J.-L.; Li, Z.-T. *Chem. Commun.* **2012**, *48*, 10999.

(20) Li, S.-H.; Zhang, H.-Y.; Xu, X.; Liu, Y. *Nat. Commun.* **2015**, *6*, 7590.

(21) Tan, L.-L.; Li, H.; Tao, Y.; Zhang, S. X.-A.; Wang, B.; Yang, Y.-W. *Adv. Mater.* **2014**, *26*, 7027.

(22) Ogoshi, T.; Sueto, R.; Yoshikoshi, K.; Sakata, Y.; Akine, S.; Yamagishi, T.-a. *Angew. Chem., Int. Ed.* **2015**, *54*, 9849.

(23) Mitra, T.; Jelfs, K. E.; Schmidtmann, M.; Ahmed, A.; Chong, S. Y.; Adams, D. J.; Cooper, A. I. *Nat. Chem.* **2013**, *5*, 276.

DOI: 10.1021/jacs.6b13300
J. Am. Chem. Soc. 2017, 139, 2908−2911